Supplementary Text.

EXPERIMENTAL PROCUDURES

Construction of rabies virus genomic and helper plasmids

Genomic RNA of SADΔG-GFP rabies virus (Wickersham et al., 2007a; Wickersham et al., 2007b) was purified with QIAamp MinElute Virus Spin Kit (QIAGEN) according to the manufacturer's instructions. Reverse transcriptase reaction (Superscript III, Invitrogen) with several different primers was carried out to obtain partial cDNA fragments of the rabies virus genome. To construct helper plasmids, which encode nucleocapsid (pcDNA-SADB19N), rabies viral RNA polymerases (pcDNA-SADB19P and pcDNA-SADB19L) or rabies glycoprotein (pcDNA-SADB19G), we amplified cDNA by the polymerase chain reaction (PCR) using primer pairs and the PCR products were inserted into the multiple cloning sites in pcDNA3.1 negative (Invitrogen).

To construct the rabies virus genomic cDNA, several pieces of rabies genomic cDNA were ligated with unique restriction enzyme sites, AgeI, MluI, BlpI, BstZ17I, and BstBI. Addition of HamRz and HdvRz sequences were performed by PCR using synthesized primers designed to attach these ribozyme sequences. The rabies genomic cDNA flanked by HamRz and HdvRz was inserted into the multiple cloning site in pcDNA3.1, becoming pcDNA-SADΔG-GFP.

Modification of the rabies genomic plasmid

The genes which replaced GFP in the pcDNA-SADΔG-GFP plasmid were amplified by PCR using plasmids encoding mCherry and primer pairs with BamHI and NheI/NotI

sequences at the ends. The ORF of mCherry-myc was obtained by inserting mCherry sequence without stop codon into pCS2+mt(Turner and Weintraub, 1994) with BamHI and ClaI site and generating a new stop codon by Klenow fill-in after EcoRI digestion. For replacement of GFP with a single gene, such as mCherry or mCherry-myc, we used BamHI at 5' and NheI for mCherry or mCherry-myc to replace GFP with one of these genes.

To generate rabies virus vectors which express two genes in different segments, we inserted the rabies transcription stop and start signals followed by mCherry ORF between the GFP stop codon and the original transcription stop signal of GFP.

5'-TAActgcagCATGAAAAAAActAACACCCCTCCactagtcgccaccATG-3'

The underlined sequences represent the transcription stop and start signals and the stop codon of GFP and the start codon of mCherry are shown at the 5' and 3' ends, respectively. Then, the partial cDNA was ligated into pcDNA-SADΔG-GFP, resulting in pcDNA-SADΔG-GFP-mCherry. Further replacement of mCherry with $ER^{T2}CreER^{T2}$ (from pCAG-$ER^{T2}CreER^{T2}$, #13777, Addgene), rtTA, or the allatostatin receptor was performed using PCR and ligation.

Design of new rabies virus plasmids

For replacement of GFP with GCaMP3, Sbf1 and PacII sequences were generated before and after GFP, respectively (pSADΔG-GFP-F2). The ORF of GCaMP3 containing Sbf1 and PacII sequences at the ends was amplified by PCR with Phusion (Finnsymes), digested with both Sbf1 and PacII, and ligated with pSADΔG-GFP-F2 digested with both Sbf1 and PacII.

To establish a two gene expression system in rabies genome, transcription stop and start sequences and 6 unique restriction enzyme sites were synthesized, annealed and ligated with pSADΔG-GFP-F2 that was digested with both Sbf1 and PacII to produce pSADΔG-F3. The pSADΔG-F3 has 3 unique restriction enzyme sites Sbf1, Srf1 and NheI for cloning the first gene and 3 unique restriction enzyme sites PacI, AscI and SacII for cloning the second gene between B19M and B19L. pSADΔG-BFP, pSADΔG-GCaMP3-DsRedX and SADΔG-FLPo-DsRedX were cloned in pSADΔG-F3. Every plasmid was sequenced before virus production.

Recovery of ΔG rabies virus

Every experimenter working with rabies viruses was vaccinated against rabies viruses and all of the experiments were conducted under BSL-2 conditions. All procedures were approved by the Salk Biosafety Committee. SADΔG-GFP, SADΔG-mCherry, SADΔG-mCherry-myc, SADΔG-mCherry-GFP, SADΔG-GFP-rtTA, and SADΔG-GFP-$ER^{T2}CreER^{T2}$ were produced using the following protocol. BSR T7/5 cells were seeded at about 50% confluency in a 6-well plate and grown in DMEM supplemented by 10% fetal bovine serum for 12 hours before the transfection. 10.0 μg of pcDNA-SADΔG-GFP or other genomic plasmids, 5.0 μg of pcDNA-SADB19N, 2.5 μg of pcDNA-SADB19P, 2.5 μg of pcDNA-SADB19L and 2.0 μg of pcDNA-SADB19G were transfected with a calcium-phosphate transfection method (ProFection® Mammalian Transfection System, Promega) following the protocols.

SADΔG-GFP, SADΔG-BFP, SADΔG-GCaMP3, SADΔG-GCaMP3-DsRedX,

SADΔG-ChR2-mCherry, SADΔG-GFP-AlstR, and SADΔG-FLPo-DsRedX were produced using the following new methods. For recovery of new variants from DNA, B7GG cells were plated onto a 60 mm dish in the absence of Antibiotic-Antimycotic in a humidified atmosphere of 5% CO_2 and 95% air at 37°C. One day later, the cells were transfected with 12.0 μg of pcDNA-SADΔG-GFP or pSADΔG-GFP-F2, 6.0 μg of pcDNA-SADB19N, 3.0 μg of pcDNA-SADB19P, 3.0 μg of pcDNA-SADB19L and 2.4 μg of pcDNA-SADB19G using Lipofectamine 2000 (Invitrogen) and OPTI-MEM (Invitrogen) in a humidified atmosphere of 3% CO_2 and 97% air at 35°C. Two days after transfection, the cells were replated onto a 100 mm dish and maintained for a week. Supernatant was collected and filtrated with 0.45 μm filter.

Amplification, pseudotyping and titration of SADΔG rabies viruses

For amplification of the recovered ΔG rabies viruses, B7GG cells were infected with SADΔG rabies viruses and maintained for 4-5 days in a humidified atmosphere of 3% CO_2 and 97% air at 35°C. For pseudotyping with EnvA, BHK-EnvA cells were infected with unpseudotyped SADΔG rabies viruses, washed with PBS, reacted with 0.25% trypsin-EDTA and replated on new dishes. Virus supernatant was collected 3-4 days after replating, filtrated with 0.45 μm filter and concentrated by two rounds of ultracentrifuge. For in vivo injection, ΔG rabies viruses were amplified in 10, 15 cm dishes in a humidified atmosphere of 3% CO_2 and 97% air at 35°C, filtrated with 0.45 μm filter and concentrated by two rounds of ultracentrifuge. Unpseudotyped rabies viruses and EnvA-pseudotyped rabies viruses were titrated with HEK293t cells and HEK293-TVA cells, respectively. In brief,

cells were seeded on 24-well plates at 1.5 x 10^5 cells per well. One day after plating, a tenfold serial dilution of virus was applied in each well. Viral titers were determined by counting florescence-expressing cells. The titers and transgene size of viruses were shown in **Table 1**. The viruses were stored at -80°C until use.

Production of HIV lentivirus

To express multiple genes under the control of a single promoter, coding sequences were linked by self-cleaving 2A sequences (Ryan and Drew, 1994; Szymczak et al., 2004). The coding sequence of Histone2B-tagged GFP was amplified by PCR to replace its stop codon with a -GSG- (Gly-Ser-Gly) linker and the F2A element, and combined with the coding sequence of rabies glycoprotein B19G containing its stop codon. The DNA region encoding EGFP in the pBOB-CMV-EGFP was replaced with a fragment encoding both Histone2B-tagged GFP and rabies glycoprotein B19G linked by the F2A element (pLenti-CMV-hGFP-F2A-B19G). HEK293t cells were plated on 6, 10 cm dishes and transfected with the pLenti-CMV-hGFP-F2A-B19G plasmid (60.0 μg) and the packaging plasmids pMDL-gp-RRE (39.0 μg), pRSV-Rev (13.0 μg) and pCMV-VSVG (21.0 μg) using Lipofectamine 2000. Transfected HEK293t cells were maintained in the presence of forskolin (10 μM) for 48 h in a humidified atmosphere of 3% CO_2 and 97% air at 35°C. Supernatants were collected, filtered with 0.45 μm filter, and concentrated by ultracentrifugation at 4°C.

Generation of B7GG cells

For generation of BHK cells expressing T7 polymerase, rabies glycoprotein B19G and GFP,

BSR T7/5 cells were infected with HIV lentivirus expressing Histone2B-tagged GFP and B19G under the control of CMV promoter in the presence of polybrene (2.0 μg/ml). After four passages, cells with high expression levels of GFP were collected with fluorescent-activated cell sorting (FACS) (**Figure S1**) as described previously (Osakada et al., 2008). FACS-sorted GFP^{high+} cells were maintained in a 100 mm dish in the presence of Antibiotic-Antimycotic (Invitrogen) for 1 week in a humidified atmosphere of 5% CO_2 and 95% air at 37°C. Expression of transgenes was confirmed by RT-PCR as previously described (Osakada et al., 2008). In brief, total RNA was extracted with RNeasy (QIAGEN) and reverse-transcribed with first-strand cDNA synthesis kit (Amersham Biosciences). The synthesized cDNA was amplified with gene-specific primers as follows: *T7 polymerase* (forward: 5'-GCTCGCGAACAGTTGGCCCT-3', reverse: 5'-GAGGCTTGGCGGCAGCGTTA-3'), *B19G* (forward: 5'-TCCCCCTTGTGCACCCCCTG, reverse: 5'-CCCCCAGTTCGGGAGACCCA-3'), *GFP* (forward: 5'-GAAGCGCGATCACATGGT-3', reverse: 5'-CCATGCCGAGAGTGATCC-3'), and *GAPDH* (forward: 5'-ACCACAGTCCATGCCATCAC-3'and reverse: 5'-TCCACCACCCTGTTGCTGTA-3'). The PCR products were separated by electrophoresis on a 2% agarose gel and detected under UV illumination.

Brain injection of rabies virus

All procedures using live animals were approved by the Institutional Animal Care and Use Committee at the Salk Institute for Biological Studies. Adult (7-9 weeks) Long-Evans rats, C57BL/6J mice and some strains of GAD-GFP mice, GIN (Oliva et al., 2000) and G30

(Lopez-Bendito et al., 2004), were used for in vivo injection of rabies viruses. Mice were anesthetized with ketamine (100 mg/kg, i.m.) and xylazine (10 mg/kg, i.m.). Long-Evans rats with ketamine (100 mg/kg, i.m.), xylazine (5.0 mg/kg, i.m.), and acepromazine (1.0 mg/kg, i.m.). Anesthetized animals were placed into a stereotaxic apparatus (David Kopf Instruments). The skull was exposed via a small incision, and a small hole was drilled for injection. Virus was loaded into glass pipettes (tip diameter, ≈ 30 μm) pulled on a P-97 micropipette puller (Sutter). Before injection of virus, the pipette was left in the brain for 5 min after penetration. Five hundreds nl of virus was injected into the following locations at a rate of 100 nL/min: dLGN (rats; 4.0 mm posterior and 4.2 mm lateral from Bregma 4.2-3.8 mm, and mice; 2.0 mm posterior and 2.0 mm lateral from Bregma and 2.5-2.2 mm depth), V1 (rats; 4.0 mm posterior and 4.2 mm lateral from Bregma 4.2-3.8 mm, and mice; 2.0 mm posterior and 2.0 mm lateral from Bregma and 2.5-2.2 mm depth), and S1 barrel cortex (mice; 1.5 mm posterior and 3.0 mm lateral from Bregma and 0.6 mm depth). After completion of the injection, the pipette was left in the brain for additional 5 min. All of the mice and rats that received injection of rabies virus variants in the brain survived and did not show abnormal behaviors. Mice that received injection of SADΔG-GFP, SADΔG-mCherry, or SADΔG-GCaMP3 appeared normal 3 months post-injection.

Two-photon imaging in SADΔG-GCaMP3- or SADΔG-GCaMP3-DsRedX-injected mice

C57BL/6J mice (5-10 weeks) were anesthetized with 1.0-1.5% isoflurane. An incision was made and the skin retracted over the stereotaxic location of V1 or V2. A metal frame was attached to the skull and the retinotopic organization of visual cortex was measured with intrinsic signal imaging through the intact skull using continuous stimulus presentation and data acquisition (Kalatsky and Stryker, 2003). Retinotopic maps from intrinsic imaging were overlaid on images of cortical surface vasculature, which allowed indentified cortical areas to be targeted for virus injection and two-photon calcium imaging. A small craniotomy was made and SADΔG-GCaMP3 was injected into the V1 of the mice at a 45 degree angle and a depth of 0.5 mm. SADΔG-GCaMP3-DsRedX was injected into the lateral extrastriate cortex (area AL; (Wang and Burkhalter, 2007)) of the mice according to the retinotopic organization, at an angle perpendicular to the brain surface, to a depth of ~0.4 mm. Nine-eleven days after virus injection, mice were again anesthetized with isoflurane, a craniotomy was made over visual cortex, covered with 1.5% agarose and a cover glass, and then sealed with Kwik-Cast. Chlorprothixene (0.5-1 mg/kg, i.m.) was administered and isoflurane was lowered to ~0.3-0.5% for visual stimulation. For visual stimulation to SADΔG-GCaMP3-injected mice, a visual stimulus consisting of drifting square-wave gratings at 8 directions in 45 degree steps (Psychtoolbox) was presented on a computer screen (100 Hz, calibrated 16” CRT) placed 10-15 cm from the animal, with 5 presentations of each grating direction in random order and a blank condition in random order. For visual stimulation to SADΔG-GCaMP3-DsRedX-injected mice, a visual stimulus

consisting of drifting square-wave gratings at 12 directions in 30 degree steps was presented on a computer screen (60 Hz, calibrated 55” LCD) placed 10-15 cm from the animal, with 5 presentations of each grating direction and a blank condition in random order. The spatial frequency of the grating was 0.04 cycles per degree (cpd) and the temporal frequency was 1 Hz. Two-photon imaging was performed using a custom-built version of the movable objective microscope (Sutter) based on a Ultrafast Ti:sapphire mode-locked laser (Chameleon Ultra, Coherent) and a laser-scanning system coupled to an upright microscope. Images were acquired using ScanImage (Pologruto et al., 2003). Time-lapse videos were processed in Matlab and ImageJ. Orientation tuning curves were generated by taking the mean response for each orientation during the entire stimulus period. Response amplitudes are presented as the relative change in fluorescence during the stimulus period compared to the prestimulus baseline (ΔF/F).

Electrophysiology in SADΔG-ChR2-mCherry- and SADΔG-GFP-AlstR-infected brain slices

SADΔG-ChR2-mCherry and SADΔG-GFP-AlstR were injected into the barrel cortex of C57BL/6J mice aged from postnatal day 8 and day 18, respectively (see above). 6-8 days postinjection, mice were anesthetized with Nembutal (100 mg/kg, i.p.) and rapidly decapitated. Coronal brain slices were cut with a vibratome at 300 μm thickness in iced artificial cerebrospinal fluid (ACSF) (24 mM NaCl, 5 mM KCl, 26 mM $NaHCO_3$, 1 mM KH_2PO_4, 1 mM $MgSO_4$, 10 mM glucose, and 1.2 mM $CaCl_2$) containing 1 mM kynurenic acid, and incubated at 35°C for at least 30 min in ACSF bubbled with 95% O_2/5% CO_2. For

recording, slices were transferred to recording chambers perfused with ACSF aerated with 95% O_2/5% CO_2 at room temperature (20–24°C). Whole-cell recordings were carried out using microelectrodes (5-7 MΩ) pulled on a P-97 micropipette puller (Sutter) from borosilicate glass (Sutter), filled with 130 mM K-gluconate, 0.2 mM EGTA, 2 mM $MgCl_2$, 6 mM KCl, 10 mM HEPES, 2.5 mM Na-ATP, 0.5 mM Na-GTP, and 10 mM K-phosphocreatine, pH 7.2, 3 mg/ml biocytin. Neurons were visualized with a differential interference contrast/fluorescent microscope (Olympus) and a video camera. Signals were amplified with a MultiClamp 700B amplifier. Data were acquired and digitized using the Spike2 Power 1401 collection system. Recorded cells were labeled with biocytin from the electrode and then processed for immunohistochemistry (see below). For photostimulation of ChR2-expressing neurons, light stimuli were delivered at 0.2-5 Hz from a blue LED (80 mW/mm^2, Asia Vital Components) that was placed above the slice at a distance of ≈ 5 mm. For inactivation of AlstR-expressing neurons, the peptide ligand AL (Ser-Arg-Pro-Tyr-Ser-Phe-Gly-Leu-NH_2) was applied by perfusion at 1 μM in ACSF. AL was washed out by replacement with normal ACSF. Spike threshold was evaluated by injection of a series of depolarizing current pulses at 750 ms duration. Input resistance was determined by injection of -200 pA current with 100 ms duration.

Biolistics on brain slice cultures

Organotypic brain slice cultures were prepared from postnatal 4- to 6-day-old Long-Evans rats as described previously (Dantzker and Callaway, 1998; Wickersham et al., 2007b). Rats were anaesthetized by hypothermia and decapitated, and brains were removed from the

skull and cut into coronal slices of 400 μm thickness. The brain slices were embedded onto a microporous membrane (Millicell-CM), placed in a six-well culture plate and maintained in a humidified atmosphere of 5% CO_2 and 95% air at 35°C. Culture medium consisting of 50% minimal essential medium/HEPES, 25% Hanks' balanced salt solution, and 25% heat-inactivated horse serum supplemented with 6.5 mg/ml glucose, 2 mM L-glutamine, 100 U/ml penicillin G potassium, and 100 μg/ml streptomycin sulfate was supplied at a volume of 1.0 ml per each well, and replaced with fresh medium every 2 days. On the next day of culture preparation, slices were transfected with the Helios Gene Gun (Bio-Rad). The following plasmids were used per 12.5 mg of gold microcarriers (1.6 μm in diameter): pCMMP-TVA800, 15.0 μg; pTetO-CMVmin-Histone2B-mCherry-F2A-rabies glycoprotein B19G, 35.0 μg. TVA800 was expressed under the control of the human cytomegalovirus (CMV) immediate-early promoter. Histone2B-tagged mCherry and rabies virus glycoprotein B19G combined with the foot-and-mouth disease virus type 2A element and GSG linker were bicistronically expressed under the tetracycline responsive promoter. One day following transfection, slices were infected with 20-50 μl of virus supernatant of EnvA-SADΔG-GFP-rtTA, and maintained in culture medium with or without doxycycline (dox, 1.0 μg/ml). Three days after virus infection, slices were fixed with 4% paraformaldehyde and then processed for immunocytochemistry.

Functional assays of rtTA, $ER^{T2}CreER^{T2}$ and FLPo rabies virus vectors

For testing SADΔG-GFP-rtTA and SADΔG-GFP-$ER^{T2}CreER^{T2}$, HEK293t cells were maintained in DMEM containing 10% FBS and transfected with a tet-responsive or Cre-

dependent plasmid using the calcium phosphate transfection method. The tet-responsive plasmid has a red fluorescent protein (DsRed monomer), under tetracycline responsive promoter after tetO promoter, six repeats of tet responsive promoters fused to a CMV minimal promoter region. The Cre-dependent plasmid pCALNL-DsRed (#13769, Addgene) expresses DsRed under the control of CAG promoter only in the presence of Cre (Matsuda and Cepko, 2007). SADΔG-GFP-rtTA, or SADΔG-GFP-ER^{T2}CreER^{T2} was used to infect the transfected cells. For induction of gene expression, 4-hydroxytamoxifen (4-HOT; 1 μM, Sigma) or doxycycline (dox; 100 nM, Sigma) were added to the culture medium.

For testing SADΔG-FLPo-DsRedX, HeLa cells stably expressing a frt-STOP-frt nuclear-localized LacZ cassette were maintained in DMEM containing 10% FBS onto poly-D-Lysine-coated 8-well culture slide (BD) in a humidified atmosphere of 5% CO_2 and 95% air at 37°C. One day after plating, SADΔG-FLPo-DsRedX was applied to the well. Two days after infection with SADΔG-FLPo-DsRedX rabies virus, cells were processed for X-gal staining. In brief, cells were fixed with 1% glutaraldehyde and 0.02% NP-40 in PBS, and reacted with 5 mM $K_4[Fe(CN)_6]$, 5 mM $K_3[Fe(CN)_6]$, 2 mM MgCl and 1 mg/ml X-gal.

Perfusion and histological analysis

Animals were deeply anesthetized 3-14 days post-injection and perfused transcardially with 4% paraformaldehyde in PBS. Brains were post-fixed with 4% paraformaldehyde in PBS and cryopreserved overnight in 2% paraformaldehyde/15% sucrose in PBS, then kept in 30% sucrose in PBS. Brains were sectioned on a freezing microtome at 40-50 μm, and stored in 30% ethylene glycol/30% glycerol/40% PBS at -20°C. Organotypic slice cultures

were fixed with 4% paraformaldehyde in PBS. Dissociated cell cultures were fixed with 4% paraformaldehyde in PBS and then processed for immunostaining.

Tissues and cells were immunolabeled as described previously (Choi et al., 2010; Osakada et al., 2008). Primary antibodies and their working dilutions were as follows: rabbit anti-GFP polyclonal (1:2000, Abcam), chicken anti-GFP polyclonal (1:500, Aves Labs), rabbit anti-DsRed polyclonal (1:400, Clontech), and preabsorbed goat anti-c-myc monoclonal (1:400, Novu). Labeled cells were visualized with the fluorescent secondary antibodies: anti-mouse IgG, anti-rabbit IgG, or anti-chicken IgY conjugated with Cy2, Cy3 (1:300, Jackson Immunoresearch), Alexa Flour 488 or Alexa Flour 594 (1:1000, Moleculer Probes). Biocytin-labeled cells were detected with streptavidin conjugated with Cy2 or Cy3 (1:1000, Jackson Immunoresearch). Cell nuclei were counterstained with 4’,6-diamidino-2-phenylindole (DAPI). Labeled cells were imaged with a fluorescent microscope (Olympus) or a confocal microscope (Leica).

Statistical analysis

Data are expressed as means ± S.E.M. All statistical analyses were performed using GraphPad PRISM version 5.0 (GraphPad Software Inc.). The statistical significance of difference was determined with one-way analysis of variance followed by Tukey’s test, or with *t*-test. Probability values less than 5% were considered significant.

References

Choi, J., Young, J.A., and Callaway, E.M. (2010). Selective viral vector transduction of ErbB4 expressing cortical interneurons in vivo with a viral receptor-ligand bridge protein. Proc Natl Acad Sci U S A *107*, 16703-16708.

Dantzker, J.L., and Callaway, E.M. (1998). The development of local, layer-specific visual cortical axons in the absence of extrinsic influences and intrinsic activity. J Neurosci *18*, 4145-4154.

Kalatsky, V.A., and Stryker, M.P. (2003). New paradigm for optical imaging: temporally encoded maps of intrinsic signal. Neuron *38*, 529-545.

Lopez-Bendito, G., Sturgess, K., Erdelyi, F., Szabo, G., Molnar, Z., and Paulsen, O. (2004). Preferential origin and layer destination of GAD65-GFP cortical interneurons. Cereb Cortex *14*, 1122-1133.

Matsuda, T., and Cepko, C.L. (2007). Controlled expression of transgenes introduced by in vivo electroporation. Proc Natl Acad Sci U S A *104*, 1027-1032.

Oliva, A.A., Jr., Jiang, M., Lam, T., Smith, K.L., and Swann, J.W. (2000). Novel hippocampal interneuronal subtypes identified using transgenic mice that express green fluorescent protein in GABAergic interneurons. J Neurosci *20*, 3354-3368.

Osakada, F., Ikeda, H., Mandai, M., Wataya, T., Watanabe, K., Yoshimura, N., Akaike, A., Sasai, Y., and Takahashi, M. (2008). Toward the generation of rod and cone photoreceptors from mouse, monkey and human embryonic stem cells. Nat Biotechnol *26*, 215-224.

Pologruto, T.A., Sabatini, B.L., and Svoboda, K. (2003). ScanImage: flexible software for operating laser scanning microscopes. Biomed Eng Online *2*, 13.

Ryan, M.D., and Drew, J. (1994). Foot-and-mouth disease virus 2A oligopeptide mediated cleavage of an artificial polyprotein. Embo J *13*, 928-933.

Szymczak, A.L., Workman, C.J., Wang, Y., Vignali, K.M., Dilioglou, S., Vanin, E.F., and Vignali, D.A. (2004). Correction of multi-gene deficiency in vivo using a single 'self-cleaving' 2A peptide-based retroviral vector. Nat Biotechnol *22*, 589-594.

Turner, D.L., and Weintraub, H. (1994). Expression of achaete-scute homolog 3 in Xenopus embryos converts ectodermal cells to a neural fate. Genes Dev *8*, 1434-1447.

Wang, Q., and Burkhalter, A. (2007). Area map of mouse visual cortex. J Comp Neurol *502*, 339-357.

Wickersham, I.R., Finke, S., Conzelmann, K.K., and Callaway, E.M. (2007a). Retrograde neuronal tracing with a deletion-mutant rabies virus. Nat Methods *4*, 47-49.

Wickersham, I.R., Lyon, D.C., Barnard, R.J., Mori, T., Finke, S., Conzelmann, K.K., Young, J.A., and Callaway, E.M. (2007b). Monosynaptic restriction of transsynaptic tracing from single, genetically targeted neurons. Neuron *53*, 639-647.

Supplementary Figure Legends.

Figure S1. Establishment of the B7GG packaging cell line for G-deleted rabies production. (A) The B7GG cell line was founded by FACS sorting to select the highest 6.2% of GFP-expressing cells following infection of BSR T7/5 cells with a lentivirus encoding both H2B-tagged GFP and rabies glycoprotein B19G. (B) RT-PCR analysis showed that B7GG cells expressed T7 RNA polymerase, B19G and GFP. BSR T7/5 cells, and in turn B7GG cells, were derived from BHK21 cells, which were used as a control. Both cell types express GAPDH.

Figure S2. Expression of mCherry in corticothalamic neurons following injections of SADΔG-mCherry into the dLGN of GFP expressing transgenic mouse lines *in vivo*.
(A) shows results from GIN mice and (B) from G30 mice. In both mouse lines the rabies-infected mCherry expressing neurons (middle panels) are easily distinguished from GFP positive inhibitory neurons (left panels). Blue is DAPI counterstain. Right panels are overlays of red, green and blue channels. Scale bars, 100 μm.

Figure S3. Immunohistochemical detection of the c-myc epitope tag on mCherry from SADΔG-mCherry-myc.
SADΔG-mCherry-myc was applied to cortical brain slice cultures. After fixation, mCherry (red) and c-myc tag (green) were detected with rabbit anti-DsRed and goat anti-myc antibodies and visualized with Cy3 and Cy2, respectively. Left panel shows red mCherry-expression with arrows indicating rabies-infected mCherry-positive neurons. Middle panel shows anti-myc staining of the same neurons, also indicated in the overlay (right panel).

Scale bars, 100 μm.

Figure S4. Monitoring of neural activity with GCaMP3-expressing ΔG rabies virus

(A) Morphology of a mouse V1 cortex neuron infected by nearby injection of SADΔG-GCaMP3. The illustration is a Z-stack of two-photon images taken at multiple depths. Fluorescent GCaMP3 can be seen through the neuron's cell body, dendrites, and dendritic spines. Scale bar, 30 μm. (B) Orientation selectivity in SADΔG-GCaMP3 rabies-infected neuron. The orientation tuning curve is plotted as the mean change in fluorescence of the cell body during the entire stimulus period, in response to square-wave gratings (0.04 cpd) presented at various orientations, and directions, drifting at 1.67 Hz. (C) Changes in fluorescence over time, in response to drifting gratings at the preferred orientation of 45 degrees. Time 0 indicates the onset of the visual stimulus, which lasted for 6 seconds, as indicated by the black bar. Values in C and D represent means ± S.E.M. of ΔF/F values across 5 repetitions of the visual stimulus.

Figure S5. Orientation selectivity in GCaMP3-DsRedX-expressing neurons in the V1.

(A, D) Two-photon laser-scanning images of SADΔG-GCaMP3-DsRedX-infected neurons at a depth of 520-535 μm 9 days after injection. SADΔG-GCaMP3-DsRedX was injected into the lateral extrastriate cortical area AL of the mice according to the retinotopic map. V1 neurons were retrogradely labeled with SADΔG-GCaMP3-DsRedX and coexpressed GCaMP3 (green) and DsRedX (red) in deep layers. Scale bar, 25 μm. (B, E) Examples of orientation selectivity recorded from 6 SADΔG-GCaMP3-DxRedX-infected V1 neurons

labeled by number in A (B1-B3) and D (E1-E3), respectively. The orientation tuning curve is plotted as the mean change in the GCaMP3 fluorescence of the soma in response to each direction of the square-wave gratings. (C, F) Changes in fluorescence over time, reflecting visual responses to drifting gratings at the preferred direction of each neuron. Stimulus duration for 4 seconds is represented by the black bar under the curve. Time 0 indicates the onset of the visual stimulus. Values in B, C, D and E represent means ± S.E.M. of ΔF/F values across 5 repetitions of the visual stimulus. (G, J) SADΔG-GCaMP3-DsRedX-infected neurons in the V1 coexpressed GCaMP3 (green) and DsRedX (red) in the same mouse imaged again on day 11. Images are at the depth of 350 μm (G, J). Scale bars, 25 μm. (H, K) Examples of orientation selectivity in SADΔG-GCaMP3-DxRedX-infected V1 neurons illustrated in G and J. GCaMP3 signals were optically recorded from 3 different neurons in each field of view shown in G (H1-H3) and J (K1-K3). Changes in the fluorescence were observed at either the soma (H1, K1: Cell 1) or the dendrites (H2, K2: Cell 2 and H3, K3: Cell 3) in response to drifting gratings. (I, L) Temporal changes in GCaMP3 fluorescence in response to drifting gratings at the preferred direction. Note that orientation and direction selectivity were detected from GCaMP3-labeled dendrites and that infected neurons clearly showed robust visual responses and orientation selectivity even 11 days after injection.

Supplementary Movie 1.

This movie illustrates changes in fluorescence of the same neuron for which data are illustrated in **Supplementary Figure 4**. SADΔG-GCaMP3 was injected into the V1 of mice

and two-photon imaging at an optical plane including the cell body was used to monitor fluorescence changes in response to visual stimuli. The 10 second duration of the movie corresponds to the same 10 second period illustrated in **Supplementary Figure 4**. In response to a drifting grating at the preferred orientation of 45 degrees, there are several clear "flashes" at the position of the cell body in the center of the image, corresponding to the times when the preferred phase of the grating is optimally positioned within the cell's receptive field.

Supplementary Movie 2.

This movie illustrates the Z-stack of images of SADΔG-GCaMP3-DsRedX-infected neurons in the V1, which correspond to **Figure 2B**. Note that the SADΔG-GCaMP3-DsRedX-labeled apical dendrites are visible from the superficial cortical layers to the point where they meet with their cell bodies in deep layers, and that neurons are visible at the deepest imaging plane at a depth of 1.5 mm from the pial surface.

Supplementary Movie 3.

This movie illustrates changes in the fluorescence of the SADΔG-GCaMP3-DsRedX-infected V1 neuron from **Figure 2C1**. GCaMP3 signals in the soma were analyzed 9 days after injection. Increase in the GCaMP3 signal (ΔF/F) is the response to the preferred direction stimulus. There are several clear "flashes" at the position of the cell body in the center of the image, corresponding to the times when the preferred phase of the grating is optimally positioned within the cell's receptive field. The time course in the movie

corresponds to **Figure 2E1**.

Supplementary Figure Legends.

Figure S1. Establishment of the B7GG packaging cell line for G-deleted rabies production. (A) The B7GG cell line was founded by FACS sorting to select the highest 6.2% of GFP-expressing cells following infection of BSR T7/5 cells with a lentivirus encoding both H2B-tagged GFP and rabies glycoprotein B19G. (B) RT-PCR analysis showed that B7GG cells expressed T7 RNA polymerase, B19G and GFP. BSR T7/5 cells, and in turn B7GG cells, were derived from BHK21 cells, which were used as a control. Both cell types express GAPDH.

Figure S2. Expression of mCherry in corticothalamic neurons following injections of SADΔG-mCherry into the dLGN of GFP expressing transgenic mouse lines *in vivo*.
(A) shows results from GIN mice and (B) from G30 mice. In both mouse lines the rabies-infected mCherry expressing neurons (middle panels) are easily distinguished from GFP positive inhibitory neurons (left panels). Blue is DAPI counterstain. Right panels are overlays of red, green and blue channels. Scale bars, 100 μm.

Figure S3. Immunohistochemical detection of the c-myc epitope tag on mCherry from SADΔG-mCherry-myc.
SADΔG-mCherry-myc was applied to cortical brain slice cultures. After fixation, mCherry (red) and c-myc tag (green) were detected with rabbit anti-DsRed and goat anti-myc antibodies and visualized with Cy3 and Cy2, respectively. Left panel shows red mCherry-expression with arrows indicating rabies-infected mCherry-positive neurons. Middle panel shows anti-myc staining of the same neurons, also indicated in the overlay (right panel).

Scale bars, 100 μm.

Figure S4. Monitoring of neural activity with GCaMP3-expressing ΔG rabies virus

(A) Morphology of a mouse V1 cortex neuron infected by nearby injection of SADΔG-GCaMP3. The illustration is a Z-stack of two-photon images taken at multiple depths. Fluorescent GCaMP3 can be seen through the neuron's cell body, dendrites, and dendritic spines. Scale bar, 30 μm. (B) Orientation selectivity in SADΔG-GCaMP3 rabies-infected neuron. The orientation tuning curve is plotted as the mean change in fluorescence of the cell body during the entire stimulus period, in response to square-wave gratings (0.04 cpd) presented at various orientations, and directions, drifting at 1.67 Hz. (C) Changes in fluorescence over time, in response to drifting gratings at the preferred orientation of 45 degrees. Time 0 indicates the onset of the visual stimulus, which lasted for 6 seconds, as indicated by the black bar. Values in C and D represent means ± S.E.M. of ΔF/F values across 5 repetitions of the visual stimulus.

Figure S5. Orientation selectivity in GCaMP3-DsRedX-expressing neurons in the V1.

(A, D) Two-photon laser-scanning images of SADΔG-GCaMP3-DsRedX-infected neurons at a depth of 520-535 μm 9 days after injection. SADΔG-GCaMP3-DsRedX was injected into the lateral extrastriate cortical area AL of the mice according to the retinotopic map. V1 neurons were retrogradely labeled with SADΔG-GCaMP3-DsRedX and coexpressed GCaMP3 (green) and DsRedX (red) in deep layers. Scale bar, 25 μm. (B, E) Examples of orientation selectivity recorded from 6 SADΔG-GCaMP3-DxRedX-infected V1 neurons

labeled by number in A (B1-B3) and D (E1-E3), respectively. The orientation tuning curve is plotted as the mean change in the GCaMP3 fluorescence of the soma in response to each direction of the square-wave gratings. (C, F) Changes in fluorescence over time, reflecting visual responses to drifting gratings at the preferred direction of each neuron. Stimulus duration for 4 seconds is represented by the black bar under the curve. Time 0 indicates the onset of the visual stimulus. Values in B, C, D and E represent means ± S.E.M. of ΔF/F values across 5 repetitions of the visual stimulus. (G, J) SADΔG-GCaMP3-DsRedX-infected neurons in the V1 coexpressed GCaMP3 (green) and DsRedX (red) in the same mouse imaged again on day 11. Images are at the depth of 350 μm (G, J). Scale bars, 25 μm. (H, K) Examples of orientation selectivity in SADΔG-GCaMP3-DxRedX-infected V1 neurons illustrated in G and J. GCaMP3 signals were optically recorded from 3 different neurons in each field of view shown in G (H1-H3) and J (K1-K3). Changes in the fluorescence were observed at either the soma (H1, K1: Cell 1) or the dendrites (H2, K2: Cell 2 and H3, K3: Cell 3) in response to drifting gratings. (I, L) Temporal changes in GCaMP3 fluorescence in response to drifting gratings at the preferred direction. Note that orientation and direction selectivity were detected from GCaMP3-labeled dendrites and that infected neurons clearly showed robust visual responses and orientation selectivity even 11 days after injection.

Supplementary Movie 1.

This movie illustrates changes in fluorescence of the same neuron for which data are illustrated in **Supplementary Figure 4**. SADΔG-GCaMP3 was injected into the V1 of mice

and two-photon imaging at an optical plane including the cell body was used to monitor fluorescence changes in response to visual stimuli. The 10 second duration of the movie corresponds to the same 10 second period illustrated in **Supplementary Figure 4**. In response to a drifting grating at the preferred orientation of 45 degrees, there are several clear "flashes" at the position of the cell body in the center of the image, corresponding to the times when the preferred phase of the grating is optimally positioned within the cell's receptive field.

Supplementary Movie 2.

This movie illustrates the Z-stack of images of SADΔG-GCaMP3-DsRedX-infected neurons in the V1, which correspond to **Figure 2B**. Note that the SADΔG-GCaMP3-DsRedX-labeled apical dendrites are visible from the superficial cortical layers to the point where they meet with their cell bodies in deep layers, and that neurons are visible at the deepest imaging plane at a depth of 1.5 mm from the pial surface.

Supplementary Movie 3.

This movie illustrates changes in the fluorescence of the SADΔG-GCaMP3-DsRedX-infected V1 neuron from **Figure 2C1**. GCaMP3 signals in the soma were analyzed 9 days after injection. Increase in the GCaMP3 signal (ΔF/F) is the response to the preferred direction stimulus. There are several clear "flashes" at the position of the cell body in the center of the image, corresponding to the times when the preferred phase of the grating is optimally positioned within the cell's receptive field. The time course in the movie

corresponds to **Figure 2E1**.

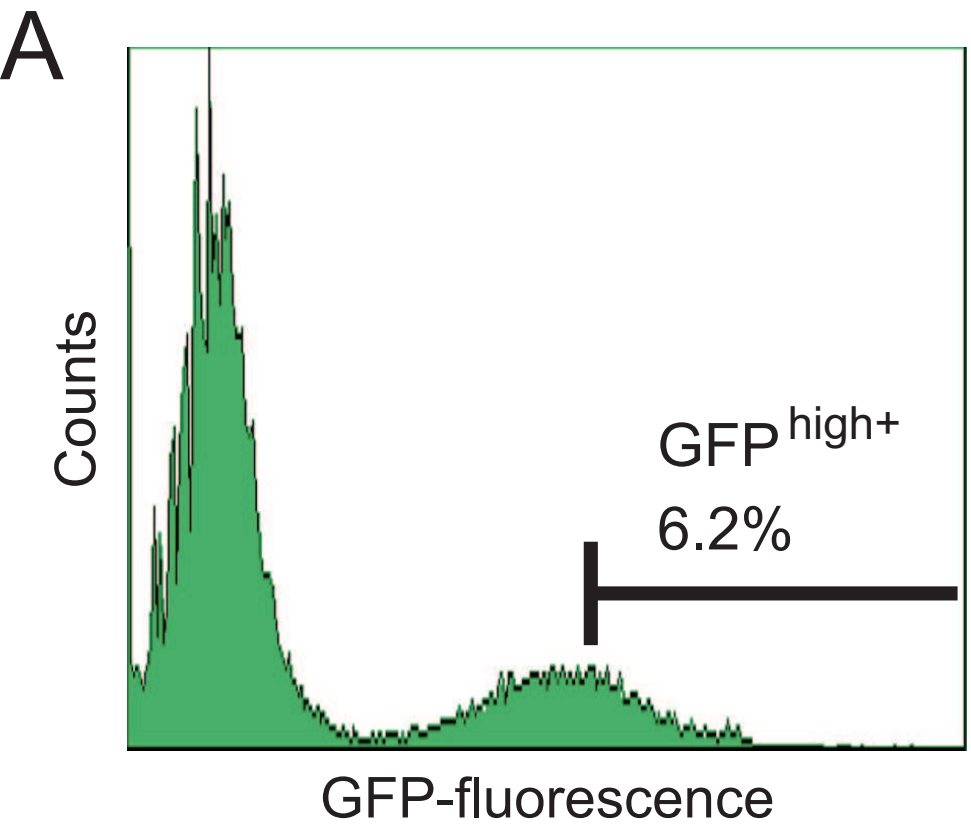

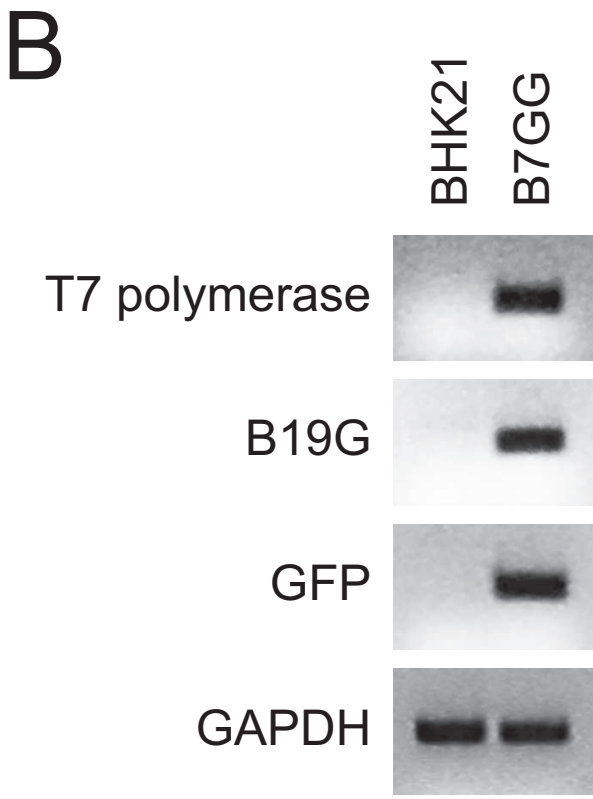

Supplementary Figure 1

Supplemental Figure 2

A GIN mouse (Oliva *et al.*, 2000)

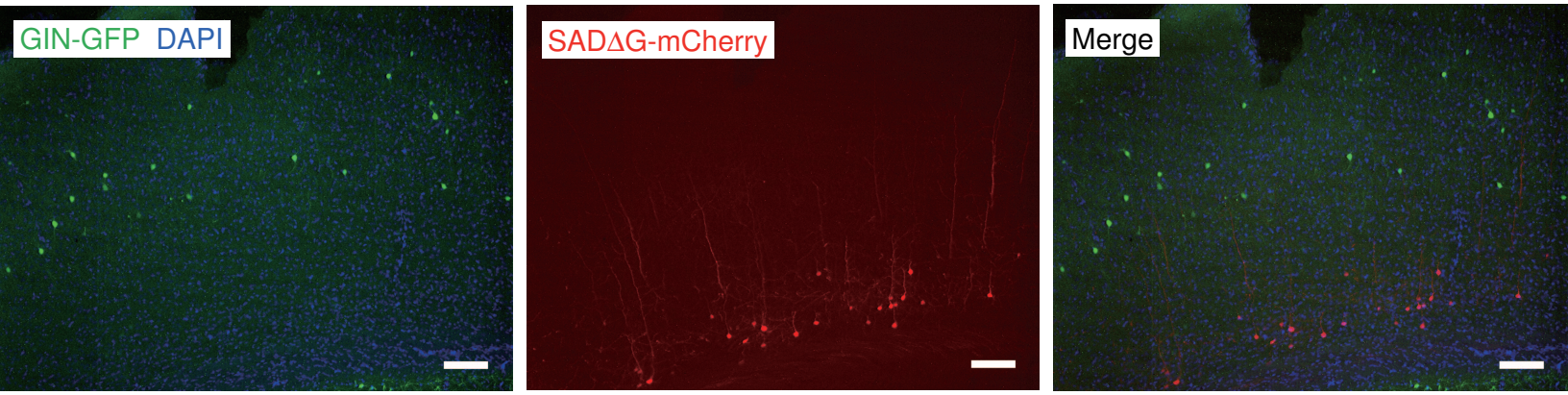

B G30 mouse (López-Bendito *et al.*, 2004)

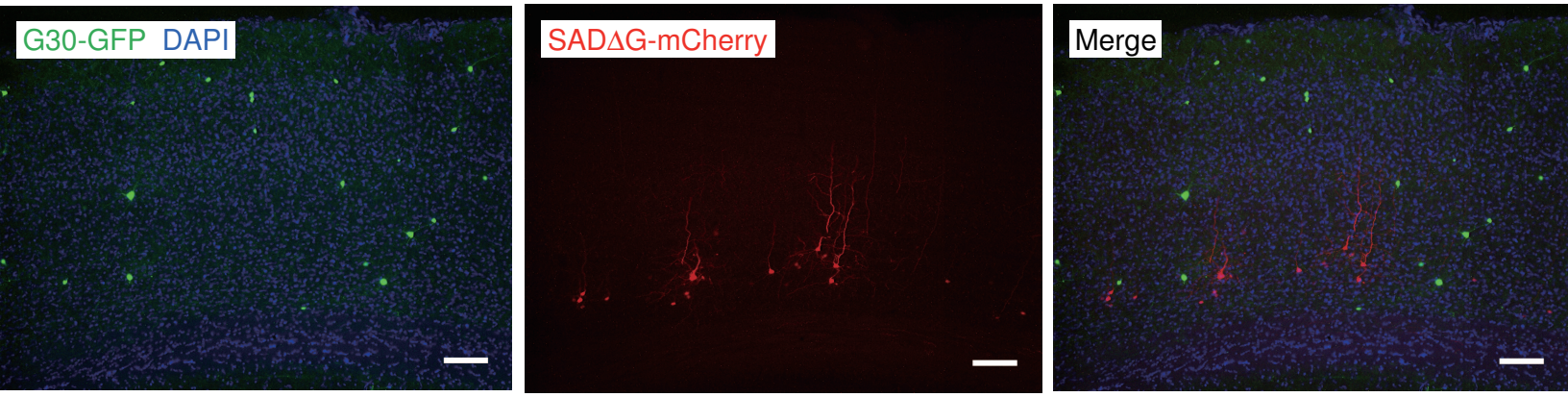

Supplementary Figure 2

Supplemental Figure 3

SADΔG-mCherry-myc

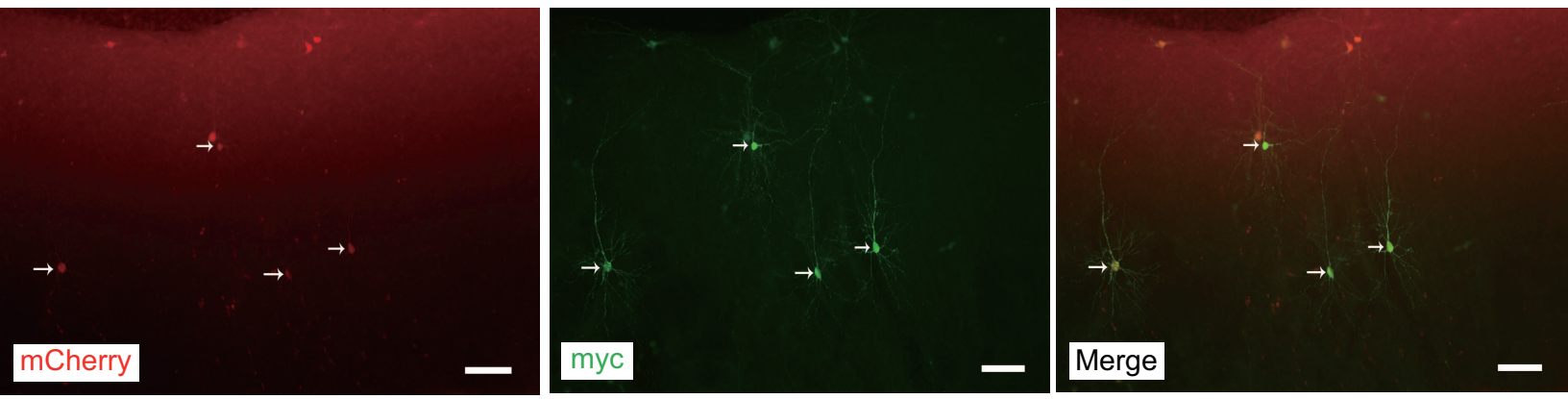

Supplementary Figure 3

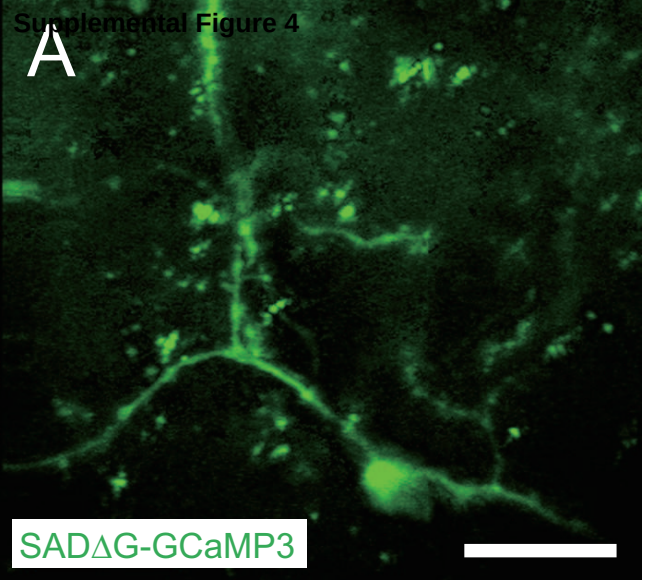

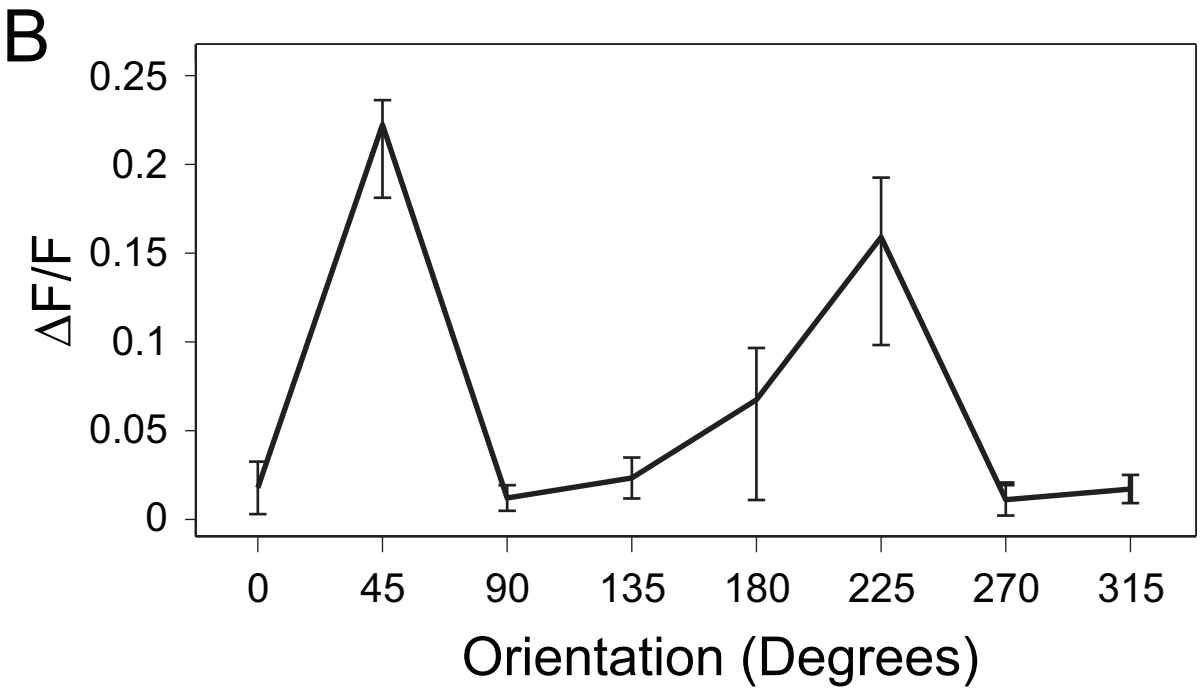

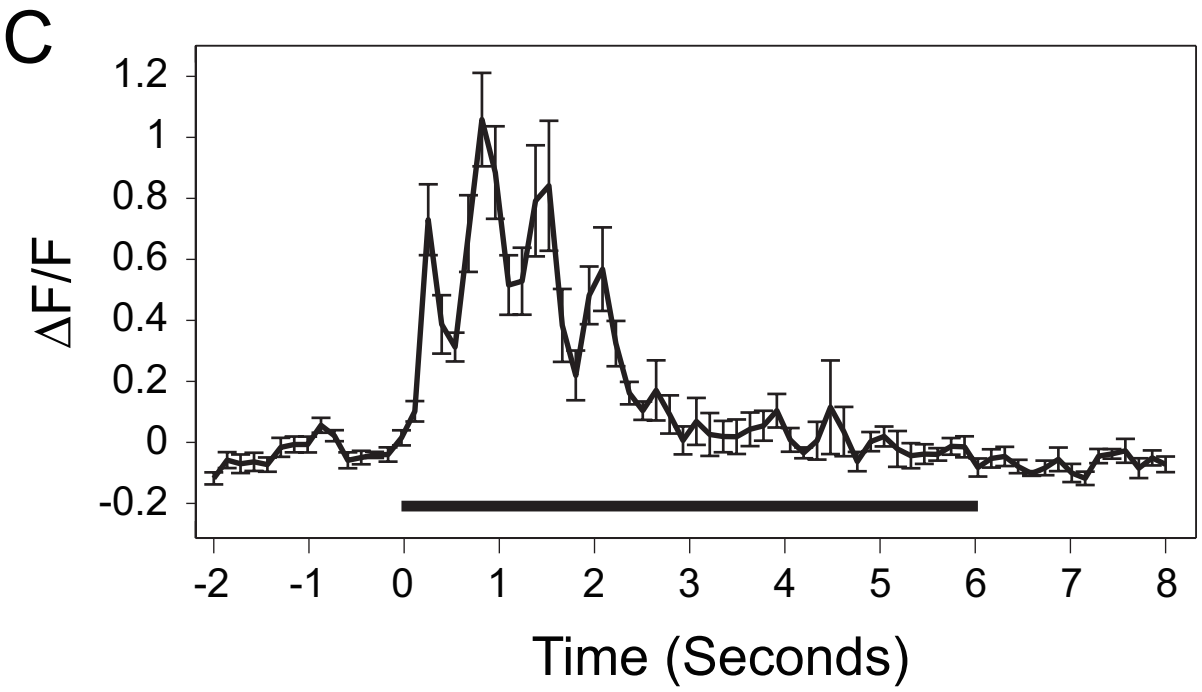

Supplementary Figure 4

Supplemental Figure 5 part 1

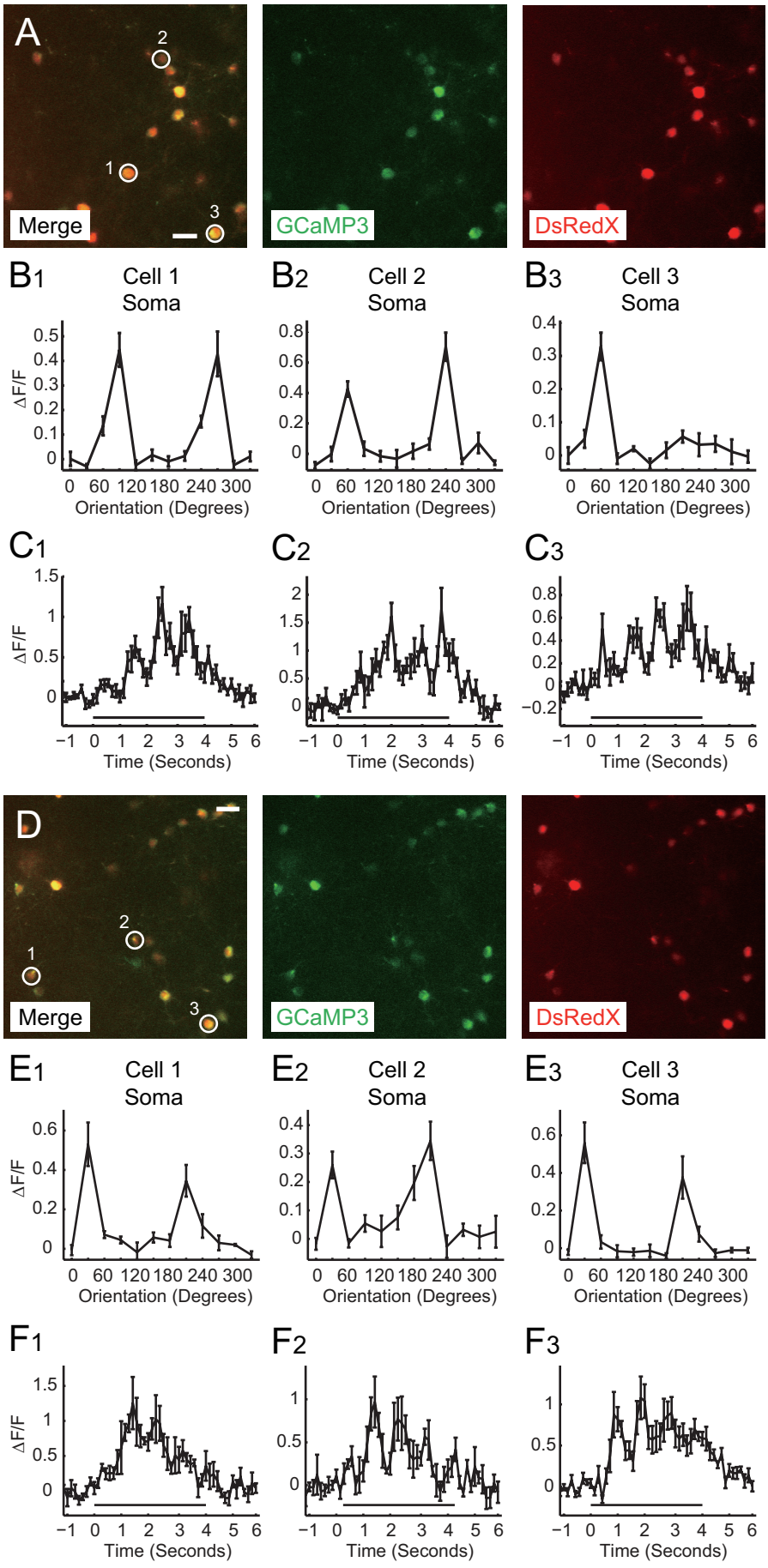

Supplementary Figure 5

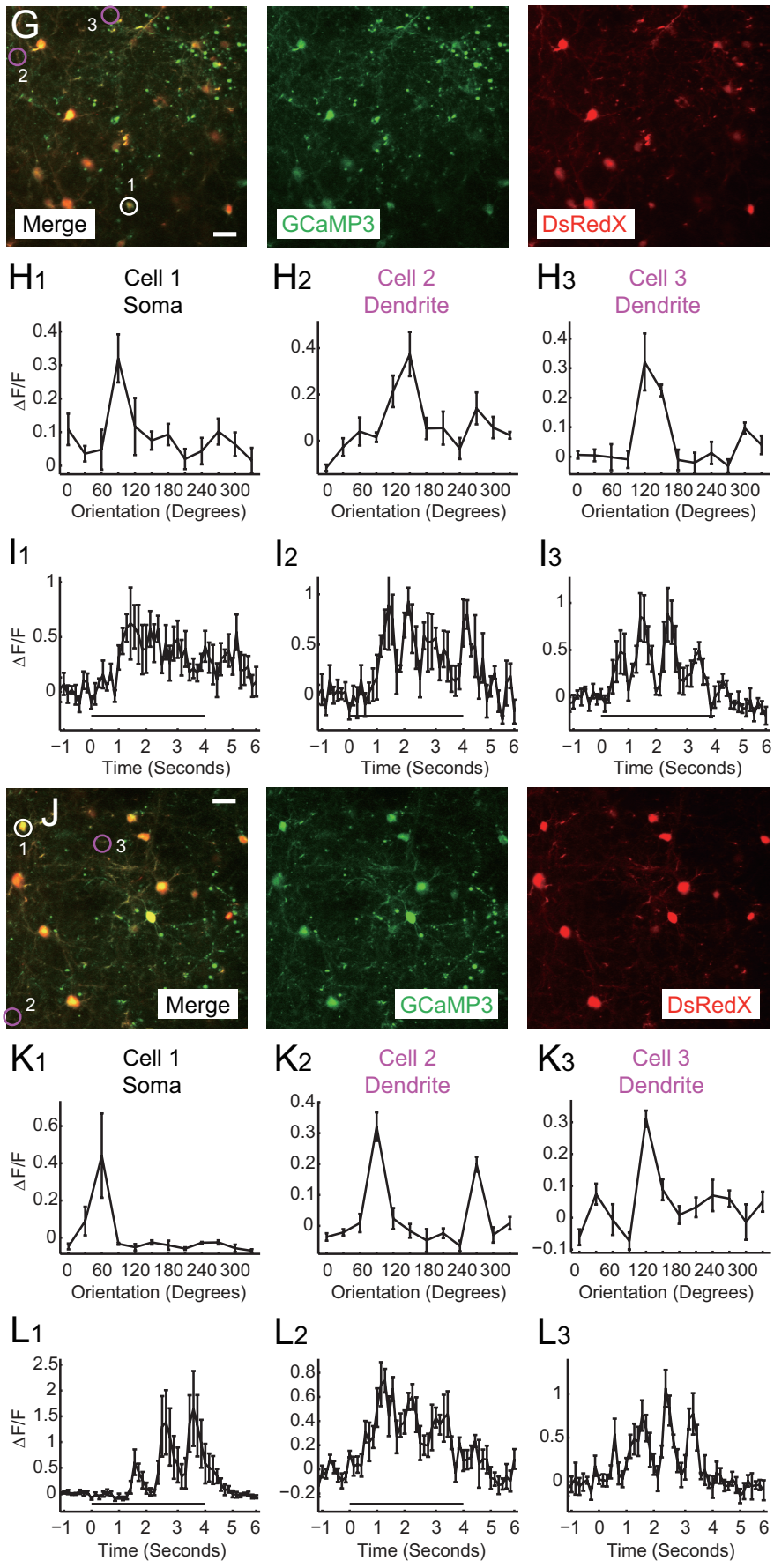

Supplementary Figure 5